

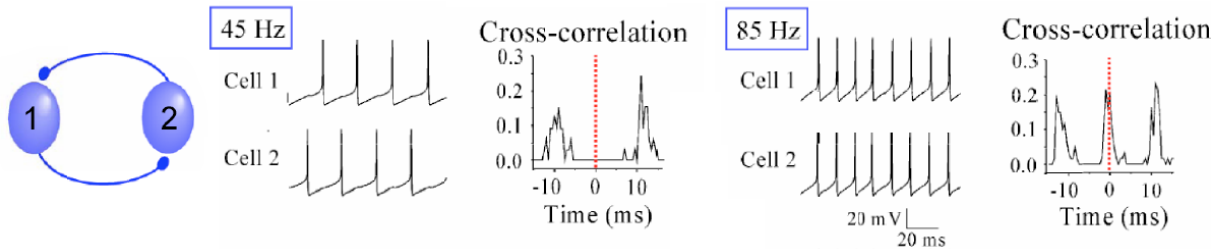
7 Circuits of Phase-Coupled Neuronal Oscillators: Applications

We return to coupled oscillators and consider a number of "realistic" scenarios in interactions that lead to the phase-locking among neurons. The first is the use of synaptic-like interactions. The second is the effect of frequency differences, with particular reference to wave generation. Finally, we consider an asymmetric system.

7.1 Classic example: Two oscillators with "low-pass", synaptic-like, coupling.

Data on the coupling of inhibitory neurons posed a challenge. Pairs of mutually inhibitory neurons locked in anti-phase at low frequencies but locked in phase at frequencies at high frequencies (Figure 1). In-phase locking with inhibition seems counterintuitive, but the interactions among oscillators are in the form of phase locking with a shift, and the shift depends on the timing of the interaction relative to the oscillation frequency.

Figure 1: A pair of PV inhibitory neurons. Data from Connors



The solution to this conundrum, proposed independently by Ermentrout and Hansel, is to consider two oscillators that interact by a synapse with a non-instantaneous rise time.

Recall the correlation integral for $\tilde{\Gamma}(\delta\psi' - \delta\psi)$ was found by subtracting the two equations of motion for the phase to get the difference, i.e.,

$$\begin{aligned}
 \frac{d(\delta\psi - \delta\psi')}{dt} &= [\Gamma(\delta\psi' - \delta\psi) - \Gamma(\delta\psi - \delta\psi')] \\
 &\equiv \tilde{\Gamma}(\delta\psi' - \delta\psi) \\
 &\equiv -\tilde{\Gamma}(\delta\psi - \delta\psi').
 \end{aligned}
 \tag{7.1}$$

The correlation integral is

$$\Gamma(\delta\psi' - \delta\psi) = \frac{\epsilon}{2\pi} \int_{-\pi}^{\pi} d\theta \vec{R}(\theta - (\delta\psi' - \delta\psi)) \cdot \vec{S}(\theta) \quad (7.2)$$

$$= \frac{\epsilon}{2\pi} \int_{-\pi}^{\pi} d\theta \vec{S}(\theta - (\delta\psi - \delta\psi')) \cdot \vec{R}(\theta) \quad (7.3)$$

Rather than choose a realistic and analytically untractable cell model, let's try some analytical methods and choose a form of $\vec{S}(\delta\psi)$ that has variable spike rate along the limit cycle. The simplest choice is

$$S(t) = \sin \omega t \quad (7.4)$$

so

$$\begin{aligned} S(\theta) &= \sin \theta \\ &= \frac{e^{i\theta} - e^{-i\theta}}{2i} \end{aligned} \quad (7.5)$$

. The interaction is given by an "α" function, i.e.,

$$R(t \geq 0) = \frac{g_{syn}}{c_m} \frac{t}{\tau} e^{-t/\tau} \quad (7.6)$$

so

$$R(\theta) = \begin{cases} 0 & \text{if } \theta < 0 \\ \frac{g_{syn}}{c_m} \left(\frac{\theta}{\omega\tau}\right) e^{-\theta/\omega\tau} & \text{if } \theta \geq 0 \\ \frac{g_{syn}}{c_m} \left[\left(\frac{\theta}{\omega\tau}\right) e^{-\theta/\omega\tau} + \left(\frac{\theta-2\pi}{\omega\tau}\right) e^{-(\theta-2\pi)/\omega\tau}\right] & \text{if } \theta \geq 2\pi \\ \text{etc.} & \end{cases} \quad (7.7)$$

We plug in and simplify the integral by assuming, to be confirmed self-consistently, that we are concerned only with values $\omega\tau \ll 2\pi$, so that only the first term in $R(\theta)$ (equation 7.7) will contribute. This means that the tail of the exponential will have well decayed over the time scale of one cycle. The upper limit can be moved from 2π to ∞ so that

$$\begin{aligned} \Gamma(\delta\psi' - \delta\psi) &= \frac{g_{syn}}{c_m} \frac{\epsilon}{2\pi} \omega\tau \int_0^{\infty} d\left(\frac{\theta}{\omega\tau}\right) \sin\left[\omega\tau\left(\frac{\theta}{\omega\tau}\right) - (\delta\psi - \delta\psi')\right] \left(\frac{\theta}{\omega\tau}\right) e^{-\theta/\omega\tau} \\ &= \frac{g_{syn}}{c_m} \frac{\epsilon}{2\pi} \omega\tau \frac{1}{2i} \left(e^{-i(\delta\psi - \delta\psi')} \int_0^{\infty} x dx e^{i\omega\tau x} e^{-x} - e^{i(\delta\psi - \delta\psi')} \int_0^{\infty} x dx e^{-i\omega\tau x} e^{-x} \right) \\ &= \frac{g_{syn}}{c_m} \frac{\epsilon}{2\pi} \omega\tau \frac{1}{2i} \left(\frac{e^{-i(\delta\psi - \delta\psi')}}{(1 - i\omega\tau)^2} - \frac{e^{i(\delta\psi - \delta\psi')}}{(1 + i\omega\tau)^2} \right) \int_0^{\infty} x dx e^{-x} \\ &= \frac{g_{syn}}{c_m} \frac{\epsilon}{2\pi} \frac{\omega\tau}{[1 + (\omega\tau)^2]^2} \left([(\omega\tau)^2 - 1] \sin(\delta\psi - \delta\psi') + 2\omega\tau \cos(\delta\psi - \delta\psi') \right) \end{aligned}$$

and thus the odd part of the interaction, relevant for pairwise interactions, is

$$\tilde{\Gamma}(\delta\psi - \delta\psi') = \frac{g_{syn}}{c_m} \frac{\epsilon}{\pi} \frac{\omega\tau [1 - (\omega\tau)^2]}{[1 + (\omega\tau)^2]^2} \sin(\delta\psi - \delta\psi') \quad (7.8)$$

so that the restoring force is

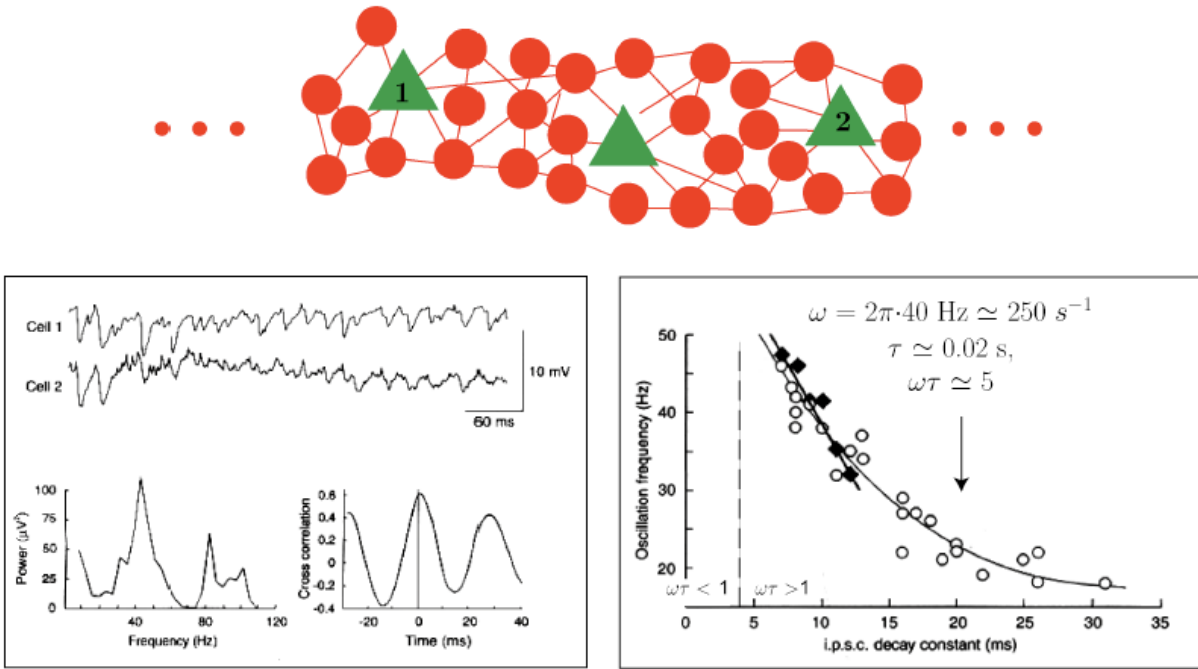
$$\left. \frac{d\tilde{\Gamma}(\delta\psi - \delta\psi')}{d(\delta\psi - \delta\psi')} \right|_{\delta\psi - \delta\psi' = 0} = \frac{g_{syn}}{c_m} \frac{\epsilon}{\pi} \frac{\omega\tau [1 - (\omega\tau)^2]}{[1 + (\omega\tau)^2]^2} \quad (7.9)$$

Recall that the "restoring force" $\left. \frac{d\tilde{\Gamma}(\delta\psi - \delta\psi')}{d(\delta\psi - \delta\psi')} \right|_{(\delta\psi - \delta\psi') = 0}$ determines the stability:

- $\left. \frac{d\tilde{\Gamma}(\delta\psi - \delta\psi')}{d(\delta\psi - \delta\psi')} \right|_{(\delta\psi - \delta\psi') = 0} > 0$ implies stability at $\delta\psi - \delta\psi' = 0$, i.e., synchrony, for excitatory connections ($g_{syn} > 0$) only for low frequencies, i.e., $\omega < 1/\tau$.
- $\left. \frac{d\tilde{\Gamma}(\delta\psi - \delta\psi')}{d(\delta\psi - \delta\psi')} \right|_{(\delta\psi - \delta\psi') = 0} > 0$ implies stability at $\delta\psi - \delta\psi' = 0$, i.e., synchrony, for inhibitory connections ($g_{syn} < 0$) only for high frequencies, i.e., $\omega > 1/\tau$.
- The result for inhibition is in agreement with the pairwise measurements of Connors (Figure 1). The situation is reversed at $\delta\psi - \delta\psi' = \pm\pi$, also in agreement with data (Figure 1). This result is also in agreement with the networks measurements of Jeffreys (Figure 2). At high frequency the entire network is synchronous, while at low frequency the oscillations cease (Figure 2), which we assume results from frustration between asynchronous

All of the action occurs near $\omega\tau = 1$, so the approximation $\omega\tau \ll 2\pi$ is justified.

Figure 2: Hippocampal slice in which all excitatory connections are blocked. The frequency is manipulated with various pharmaceutical agents. Data from Whittington, Traub and Jeffreys 1995



A final point is that phase-locking is accompanied by a shift in frequency, found from the "even" part of $\Gamma(\delta\psi - \delta\psi')$, i.e., the *cosine* term in Equation 7.8. For the present case the shift is

$$\Delta\omega = \frac{g_{syn}}{c_m} \frac{\epsilon}{2\pi} \frac{(\omega\tau)^2}{[1 + (\omega\tau)^2]^2}. \quad (7.10)$$

The sign of the shift depends on that of g_{syn} but is independent of $\omega\tau$. The magnitude of the shift peaks at $\omega\tau = 1$.

7.2 Two oscillators with different intrinsic frequencies.

We take

$$\Gamma(\theta) \equiv -\Gamma_0 \sin(\theta). \quad (7.11)$$

Then a system with two coupled neuronal oscillators with different intrinsic frequencies can be expressed as

$$\frac{d\delta\psi}{dt} = \delta\omega + \Gamma_0 \sin(\delta\psi' - \delta\psi) \quad (7.12)$$

and

$$\frac{d\delta\psi'}{dt} = \delta\omega' + \Gamma_0 \sin(\delta\psi - \delta\psi'). \quad (7.13)$$

Subtracting these gives

$$\begin{aligned} \frac{d(\delta\psi - \delta\psi')}{dt} &= (\delta\omega - \delta\omega') + \Gamma_0 \sin(\delta\psi' - \delta\psi) - \Gamma_0 \sin(\delta\psi - \delta\psi') \\ &= (\delta\omega - \delta\omega') - 2\Gamma_0 \sin(\delta\psi - \delta\psi'). \end{aligned} \quad (7.14)$$

The system will phase lock, for which $\frac{d\delta\psi}{dt} = \frac{d\delta\psi'}{dt}$, so long as the interaction strength, i.e.,

$$\tilde{\Gamma} = 2\Gamma_0 \sin(\delta\psi - \delta\psi') \quad (7.15)$$

balances the difference in frequencies, i.e.,

$$2\Gamma_0 \sin(\delta\psi' - \delta\psi) = \delta\omega' - \delta\omega. \quad (7.16)$$

This requires

$$\frac{2\Gamma_0}{|\delta\omega - \delta\omega'|} > 1 \quad (7.17)$$

and the phase shift between the peak activity in the two neurons is just

$$\delta\psi - \delta\psi' = \sin^{-1} \left(\frac{\delta\omega - \delta\omega'}{2\Gamma_0} \right). \quad (7.18)$$

The oscillator with the higher intrinsic frequency leads. The frequency under phase lock, found by adding the equations, is

$$\omega_{observed} = \omega + \frac{\delta\omega + \delta\omega'}{2}. \quad (7.19)$$

$\delta\psi - \delta\psi'$ and $\omega_{observed}$ are the two quantities that are measured in the laboratory.

Box 1. Quasiperiodic motion when locking does not occur

Outside of the phase locked region one must integrate the equations of motion, i.e.,

$$\int_0^{\delta\psi - \delta\psi'} \frac{dx}{(\delta\omega - \delta\omega') - 2\Gamma_0 \sin x} = \int_0^t dt'. \quad (7.20)$$

which, from tabulated integrals, is

$$\delta\psi - \delta\psi' = -2 \tan^{-1} \left[\frac{2\Gamma_0 + \sqrt{(\delta\omega - \delta\omega')^2 - 4\Gamma_0^2} \tan \left(\frac{\sqrt{(\delta\omega - \delta\omega')^2 - 4\Gamma_0^2}}{2} t \right)}{\delta\omega' - \delta\omega} \right]. \quad (7.21)$$

The system undergoes quasiperiodic motion as the phase difference evolves with a period of

$$T_{\delta\psi - \delta\psi'} = \frac{2\pi}{\sqrt{(\delta\omega - \delta\omega')^2 - 4\Gamma_0^2}} \quad (7.22)$$

and, near locking, maintain a near constant phase difference of $\pi/2$ until the two oscillators rapidly slip once every period.

Box 2. Chain of oscillators with $\delta\omega \propto \Delta x$

$$\frac{d\delta\psi_x}{dt} = \delta\omega_x + \sum_{x \neq x'} \Gamma(\delta\psi_x - \delta\psi_{x'}) \quad (7.23)$$

with

$$\delta\omega_x \propto x + \text{constant}. \quad (7.24)$$

When the system locks, there can be many strings of oscillators, each with the same frequency (Figure 3). For strong enough interaction, all oscillators lock at the same frequency, but a gradient of phase shifts with $\frac{\Delta\psi_x}{dx}$ given by a monotonic function of x , like $\frac{\Delta\psi_x}{dx} \propto \text{constant}$, i.e., the phase shift appears as a traveling wave. The data on electrical waves from Limax olfaction shows traveling waves and a gradient of intrinsic frequencies.

7.3 Unidirectional coupling: One oscillator drives another.

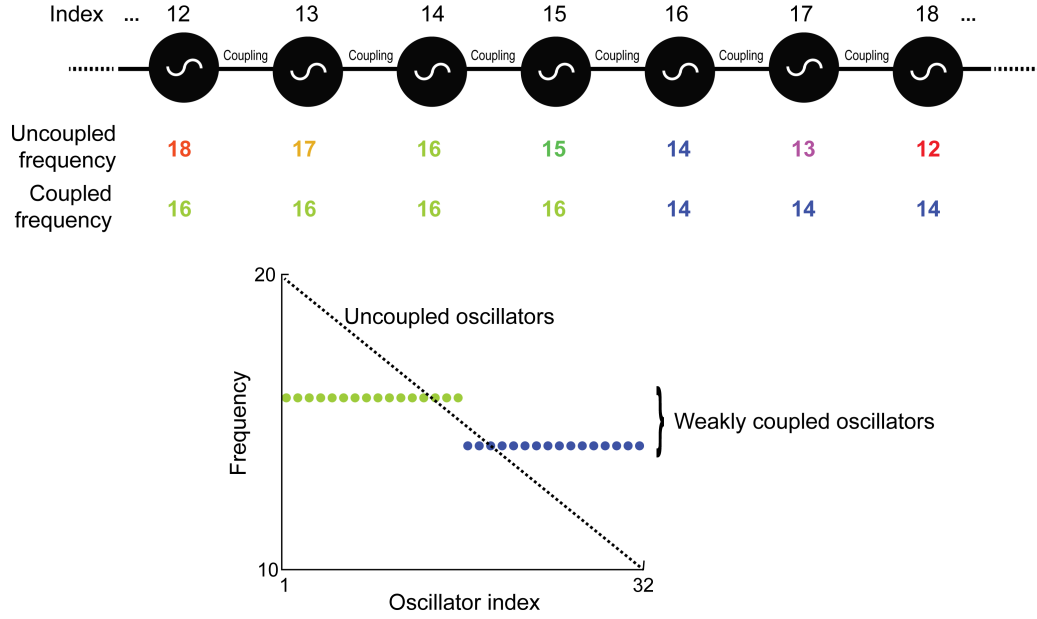
A common situation, and our last example, is that of one oscillator attempting to entrain another. Here the coupling is unidirectional. Let the external drive have frequency ω_D and coupling strength Γ_D with a phase $\psi'(t)$ defined by

$$\frac{d\psi'(t)}{dt} = \omega_D \quad (7.25)$$

Then a simple formalism for the phase of the driven oscillator, with intrinsic frequency ω_o , is of the form

$$\frac{d\psi(t)}{dt} = \omega + \Gamma_D \sin(\psi'(t) - \psi(t)) \quad (7.26)$$

Figure 3: Parcellation in one dimensional lattice of weakly coupled oscillators. From Ermentrout and Kopell, 1984



$$= \omega + \Gamma_D \sin(\omega_D t + \psi_o - \psi(t))$$

where ψ_o is a phase shift. In steady state

$$\frac{d\psi(t)}{dt} = \omega_D. \quad (7.27)$$

Substituting in gives a phase shift of

$$\psi - \psi_o = \sin^{-1} \left(\frac{\omega_D - \omega}{\Gamma_D} \right). \quad (7.28)$$

We see that locking can occur only for $\omega - \Gamma < \omega_D < \omega + \Gamma$ and that the faster oscillator is phase advanced.

Box 3 .Phase-coupled oscillators are not driven harmonic oscillators

The behavior of driven phase-coupled oscillators behavior is quite different from that for a linear (harmonic) oscillator governed by the equation

$$\frac{d^2 x(t)}{dt^2} + \omega_o^2 x(t) + \beta \frac{dx(t)}{dt} = A \cos(\omega_D t), \quad (7.29)$$

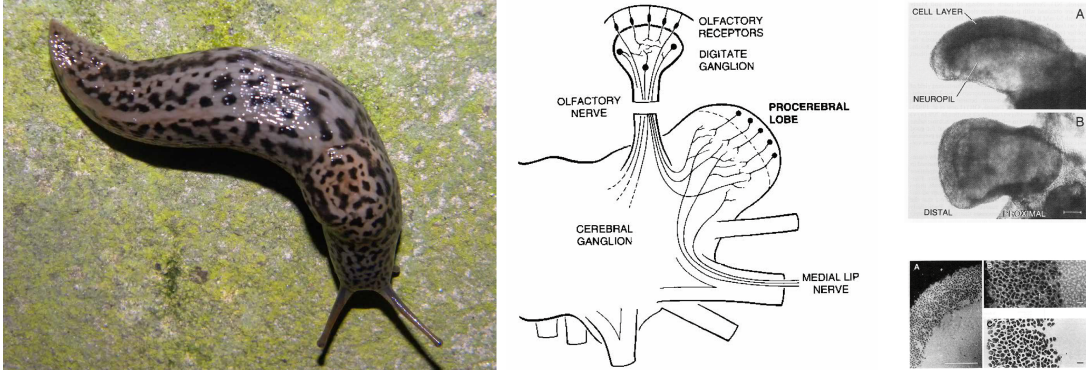
where β is a loss term. This has the well know steady-state solution

$$x(t) = \frac{A}{\sqrt{(\omega_D^2 - \omega_o^2)^2 + \beta^2 \omega_D^2}} \cos \psi(t), \quad (7.30)$$

with

$$\psi(t) = \omega_D t - \psi_1 \quad (7.31)$$

Figure 4: The olfactory system of the mollusc *Limax maximus*. From Delaney, Gelperin, Fee, Flores, Gervais, Tank and Kleinfeld, 1994



and phase shift

$$\psi_1 = \tan^{-1} \left(\frac{\beta \omega_D}{\omega_D^2 - \omega_o^2} \right). \quad (7.32)$$

Here, the maximum phase-shift swings over a maximum range of $\psi_1 = 0$ to $\psi_1 = \pi$ as the drive frequency is swept from $\omega_D = 0$ to $\omega_D \rightarrow \infty$. Amplitude issues aside, the range is the same as the nonlinear oscillator but the dynamics are quite different.

Box 3. Case of quasiperiodic motion of driven oscillators When the interaction is too weak for locking, there is a time-varying phase shift between the drive and the driven oscillator. We write

$$\psi(t) = x(t) + \omega_D t \quad (7.33)$$

so that Equation 7.27 becomes

$$\frac{dx(t)}{dt} = \omega_o - \Gamma_D \sin(x) \quad (7.34)$$

and can be directly integrated to give (using tables)

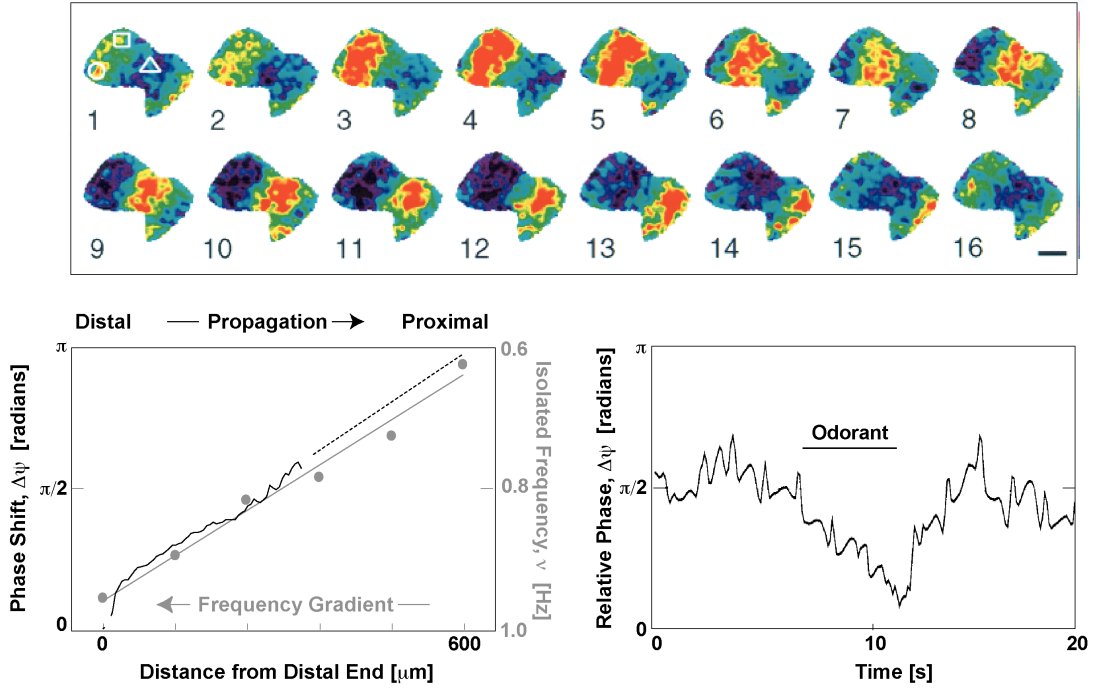
$$x(t) = 4\pi \tan^{-1} \left[\frac{\Gamma_D + \sqrt{(\omega_D - \omega_o)^2 - \Gamma_D^2} \tan \left(\frac{\sqrt{(\omega_D - \omega_o)^2 - \Gamma_D^2}}{4\pi} t \right)}{\omega_D - \omega_o} \right]. \quad (7.35)$$

The system undergoes quasiperiodic motion as the phase difference evolves with a radian frequency of

$$\Omega = \frac{\sqrt{(\omega_D - \omega_o)^2 - \Gamma_D^2}}{2\pi}. \quad (7.36)$$

Near locking, the drive maintains a near constant phase difference of $\pi/2$ until the two oscillators rapidly slip by nearly 2π once every period of $2\pi/\Omega$.

Figure 5: Propagating waves in the olfactory lobe of the mollusc *Limax maximus*. From Delaney, Gelperin, Fee, Flores, Gervais, Tank and Kleinfeld, 1994



7.3.1 Neurons driving pial arterioles.

We consider the example of neuronal local field potentials, with a roughly 0.1 Hz oscillation, that unidirectionally drive pial oscillators with a similar frequency (Figure 6); the phase shift is roughly $\pi/5$ radians.

Years back, Wiener proposed that locking could entrain a fraction of a population of driven oscillators within a range of frequencies close to the driven frequency, but did not lock oscillators too far away in frequency. This "burns a hole", as analyzed by Kuromoto (Figure 7). This prediction is now qualitatively seen between neurons and pial oscillators, where locking can occur up to 0.2 Hz (Figure 8).

Figure 6: The local field potential and pial arteriole diameter measured in mouse cortex. Note the correlation that indicated locking with a slight phase shift. From Mateo, Knutsen, Tsai, Shih and Kleinfeld, 2017

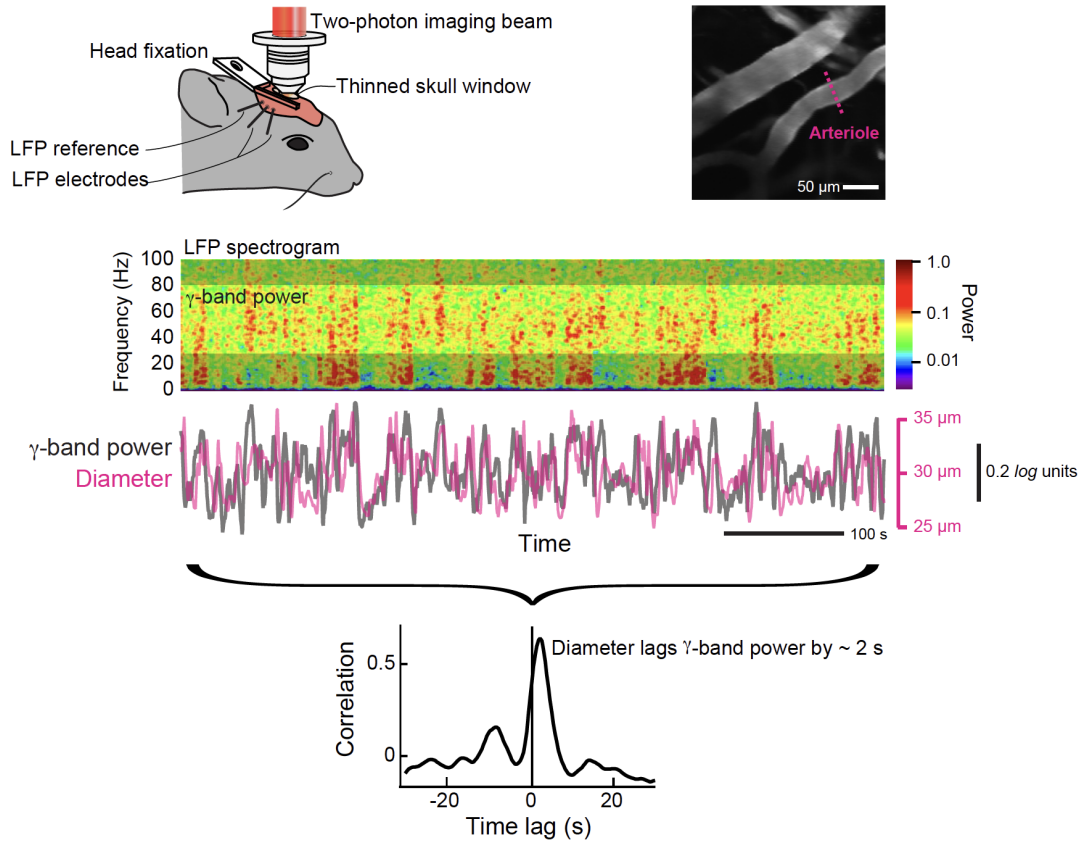


Figure 7: Cartoon from Kuromoto, 1984

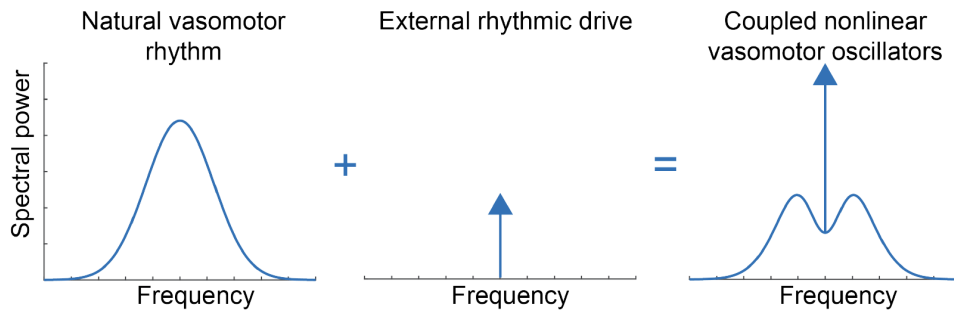


Figure 8: Locking of pial vessels in vibrissa cortex to driven vibrissa input from 0.02 to 0.5 Hz . From Brogini and Kleinfeld, unpublished

